CFD SIMULATION OF TIDAL CURRENT FARM BY USING AL MODEL

CHENG LIU[1], CHANGHONG HU[2]
[1,2] Research Institute for Applied Mechanics, Kyushu University, [1] liu@riam.kyushu-u.ac.jp,
[2] hu@riam.kyushu-u.ac.jp

Keywords: *Tidal current farm; Immersed boundary method; Wall function model; Adaptive mesh refinement; Actuator line model.*

Introduction

Tidal current power is one of the most potential resources for future electricity generation, corresponding investigation is attracted increasing interest. Mycek et al. [1] performed experiments for two tandem horizontal-axis tidal turbines (HATTs) in the IFREMER circulation flume tank, in which two ambient turbulence intensity (TI) rates (3% and 15%) is measured. Stallard et al. [2] carried out experiments to study the wake induced by staggered and aligned configurations, the wall effect was also under investigation.

Compared with experiment, numerical simulation has the potential to study the effect of different conditions with significantly lower cost. The Large Eddy Simulation (LES) and Reynolds-averaged Navier–Stokes (RANS) turbulence models can be used for predicting the mean performance and near-wake structure of a HATT. However, 3D blade-resolved simulation is cumbersome since a lot of time must be spent to generate mesh resolving the blade surface. Besides, the cost for adjusting the grid is also too high to perform numerous case-studies of a tidal farm.

In this study, an efficient numerical method for predicting the wake interference of multiple turbines is presented. To save the cost, the (actuator line) AL model [3] instead of the fully resolved turbine are developed. The URANS equations are solved to model the turbulent flow behind the rotor. Three turbulence models, original $k-\omega$, $k-\omega-SST$ and corrected $k-\omega$ model are implemented for comparison. The AL model with corrections to volume force calculation is introduced to represent the rotors. The moving least square (MLS) immersed boundary (IB) method [4] [5] considering the wall functions is proposed to study the hub and tower effect. The local mesh refinement is applied at the regions containing high gradient. The combination of AL model and IB method is highly efficient for case-studies of different configurations of multiple turbines. Numerical tests show the efficiency and accuracy for present solver in predicting velocity deficit and TIs. Present AL/MLS-IB method is also applicable for LES simulations. An example is given lastly for illustration of its potential in LES simulation of a tidal farm.

Numerical Method

Immersed Boundary Method

To impose the boundary conditions sharply around the surface, a MLS-IB method [4] [5] is applied to reconstruct the velocity at the forcing points adjacent to the rigid boundary. The fluid points, solid points and forcing points are shown as in Figure. 1 (a).

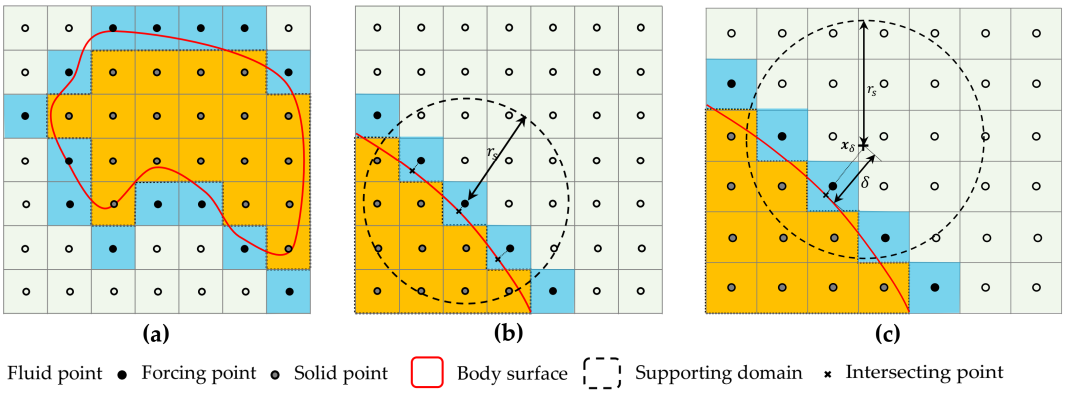

Figure 1: (a). Classification of the points in the computational domain, (b) definition of the supporting domain, (c) illustration for wall conditions of tangential velocity at the forcing points.

For present direct forcing method, the scalar quantity $\varphi(\boldsymbol{x})$ at the forcing point is determined by the moving least square approach with a supporting domain, see Fig. 1 (b),

$$\varphi(\boldsymbol{x}) = \sum_{i=1}^{m} p_i(\boldsymbol{x})\, C_i(\boldsymbol{x}) = \mathbf{p}^{\mathrm{T}}(\boldsymbol{x})\mathbf{C}(\boldsymbol{x}), \quad (1)$$

where $\mathbf{p}^{\mathrm{T}}(\boldsymbol{x})$ is the orthogonal basis function vector. The accuracy of the interpolation depends on the vector length m. $\mathbf{C}(\boldsymbol{x})$ is the coefficient vector, which can be determined by minimizing the following weighted residual,

$$\mathcal{R} = \sum_{j=1}^{n} W(\boldsymbol{x} - \boldsymbol{x}_j)\, [\mathbf{p}^{\mathrm{T}}(\boldsymbol{x}_j)\mathbf{C}(\boldsymbol{x}) - \varphi(\boldsymbol{x}_j)]^2, \quad (2)$$

where $\boldsymbol{x}_j$ stands for the fluid point and intersecting point fall into the supporting domain. n is the number of points used for reconstruction. $W(\boldsymbol{x} - \boldsymbol{x}_j)$ is the weighed function that depends on the distance between $\boldsymbol{x}$ and $\boldsymbol{x}_j$. By solving Eq. (2), the coefficients vector $\mathbf{C}(\boldsymbol{x})$ can be determined. Finally, the scalar quantity φ at the forcing point $\boldsymbol{x}$ can be calculated through Eq. (1). Details are described in [4] [5].

Wall Functions

When the turbulence flow approaches a solid wall, the mean and fluctuating components decrease quickly and create a large gradient near the wall. To accurately represent the near wall boundary layer, numerous grid points in the near wall region are required. For high Reynolds number turbulence models such as $k-\varepsilon$ and $k-\omega$ model, traditional IB method cannot fully resolve the boundary layers, the calculation of the shear stress in this way may result in incorrect values. In previous research, linear and quadratic interpolations are often been used in IB methods. However, they are effective only when the forcing points are located in the linear region of the boundary layer. In present research, by using the wall models, the logarithmic laws are maintained with medium fine resolution of the near wall layer.

For the implementation, first we should know whether the forcing point is applicable for using the wall model function. Here we use d_C^+ to determine whether the points lies in the viscous or inertial sub-layer.

$$d_C^+ = \frac{C_\mu^{0.25}\, k_C^{0.5}}{\nu}\,\mathrm{dist}(\boldsymbol{x}_c), \tag{3}$$

where ν is the laminar viscosity, k_C is the near wall turbulence kinetic energy and the function $\mathrm{dist}(\boldsymbol{x}_c)$ indicates the distance to the wall. It is assumed that the transition from the viscous region to inertia layer occur at d_{tr}^+, $d_{tr}^+ = 11$ is adopted according to previous research. The intersection position of the logarithmic and the linear profile can be represented by d_{tr}^+. For d_C^+ lower than d_{tr}^+, the forcing point C locates in the viscous region. In this case, the flow is assumed to be laminar and the viscosity at C is equal to the laminar viscosity μ. The turbulence kinetic energy k at the interface is zero, thus the MLS interpolation in Eq. (1) can be applied for the reconstruction of k at the forcing point. When $d_C^+ > d_{tr}^+$, the forcing point C is in the inertia boundary layer, so the logarithmic wall function is applied. The velocity profile of tangential component is given in the following formula through experimental investigations [9].

$$\frac{u^t}{u_\tau} = \frac{1}{\kappa}\ln(1+\kappa y^+) + 7.8\left[1 - e^{\left(\frac{-y^+}{d_{tr}^+}\right)} - \frac{y^+}{d_{tr}^+}e^{\left(\frac{-y^+}{3}\right)}\right], \tag{4}$$

here u^t is the tangential velocity, u_τ represents the friction velocity, κ is set by 0.4187. y^+ is the dimensionless wall distance. By using Eq. (4), the linear viscous sub-layer and the logarithmic layer can be replicated correctly. The wall conditions of tangential velocity at the forcing points are calculated as described in following procedure. 1. Using MLS interpolation (Eq. (1)) to obtain the tangential velocity u_δ^t at $\boldsymbol{x}_\delta$, here the distance (δ) from $\boldsymbol{x}_\delta$ to the solid surface is set by $\delta = \sqrt{2}\Delta h$, h is the grid interval, see Fig. 2. 2. Using Eq. (4) to get the friction velocity u_τ at $\boldsymbol{x}_\delta$. 3. Calculate the tangential velocity u^t using Eq. (4) again at the forcing point with the assumption that the friction velocity at the forcing point and $\boldsymbol{x}_\delta$ is identical. It is noted that in the MLS interpolation of step 1, the forcing points fall into the supporting domain should be avoided to be used. For the normal components of the velocity and other scalar qualities, the MLS interpolation is applied to reconstruct the status. In the $k-\omega$ model, the turbulence frequency ω at the forcing point can be calculated using the analytical solution. If the forcing point lies in viscous layer,

$$\omega_C = \frac{6\nu}{C_{\beta 1}\left(d_C^+\right)^2}. \tag{5}$$

Otherwise, when the forcing points in the inertia region, the ω equation will not be solved for the first interior point and the value is set by the formula,

$$\omega_C = \frac{k_C^{0.5}}{\kappa C_{\beta 1}^{0.25}\, d_C^+}. \tag{6}$$

Actuator Line Model

The AL approach is a combination of classical BEM theory and Navier–Stokes equation [3]. It is an efficient approach that can provide majority wake flow characteristics of a rotating turbine. In AL approach, the rotor is defined in Cartesian coordinate frame with three actuator lines to represent rotating blades. A series of points along each blade's axis are defined and each point is the center of an actuator element. The position of these points rotate according to the angular speed of the turbine at each time step. The critical point in implementing AL model is to add the force terms at the right side of the Navier–Stokes equation to represent the rotor effect.

Adaptive Mesh Refinement

In OpenFOAM, the adaptive mesh refinement is included in the class dynamicRefineFvMesh. By including the corresponding libraries, we can create a solver that containing AMR functions by modifying existing Foam solvers. The gradient of the velocity field is calculated to build a refinement criterion.

Numerical Solutions

URANS simulation-IFREMER rotor test

In order to validate the new developed AL model, the experimental data of the HATT model test by Mycek et al [1] is used for comparison. The experiment was carried out in the *IFREMER* flume tank, Boulogne-Sur-Mer, France in which the 1/30 scaled prototypes tidal turbine with different inlet TIs are studied. In the experiment, the upstream conditions,

$U_\infty = 0.8m/s$, $I_\infty = 3\%$ are considered. The optimized tip speed ratio (TSR) is 3.67 for all of the *IFREMER* rotor test. Other parameters, initial conditions and boundary conditions are found in reference [1].

The results of downstream turbine under low TI ($I_\infty = 3\%$) cases are shown in Figure. 2 in which the wake profiles of 7 transects (2D~10D behind the rotor plane) are given. Since the rotor is placed in the turbulent flow generated by the upstream rotor, the actual ambient TI around the downstream is larger than single turbine case. It is observed the TI profiles predicted by the $k-\omega$ model are not consistent with experiment at x/D < 3 (Figure. 2 (a)). The corrected $k-\omega$ model seems to resolve the TI profiles better around the rotor hub (x/D=2) but still give over-predict TI. For x/D > 4, the differences of the three models are not obvious. Generally, the corrected $k-\omega$ and the $k-\omega-SST$ model shows better performance in predicting TI in the near wake region, the performance of the three models are almost identical for far wake (x/D > 3). Since $k-\omega-SST$ give the lowest TI predictions, the largest velocity deficits can also be observed. To make a clearer view of the differences among the three models, the wake profiles ($I_\infty = 3\%$, 4D) along the rotor center are given as in Figure. 2 (c-d).

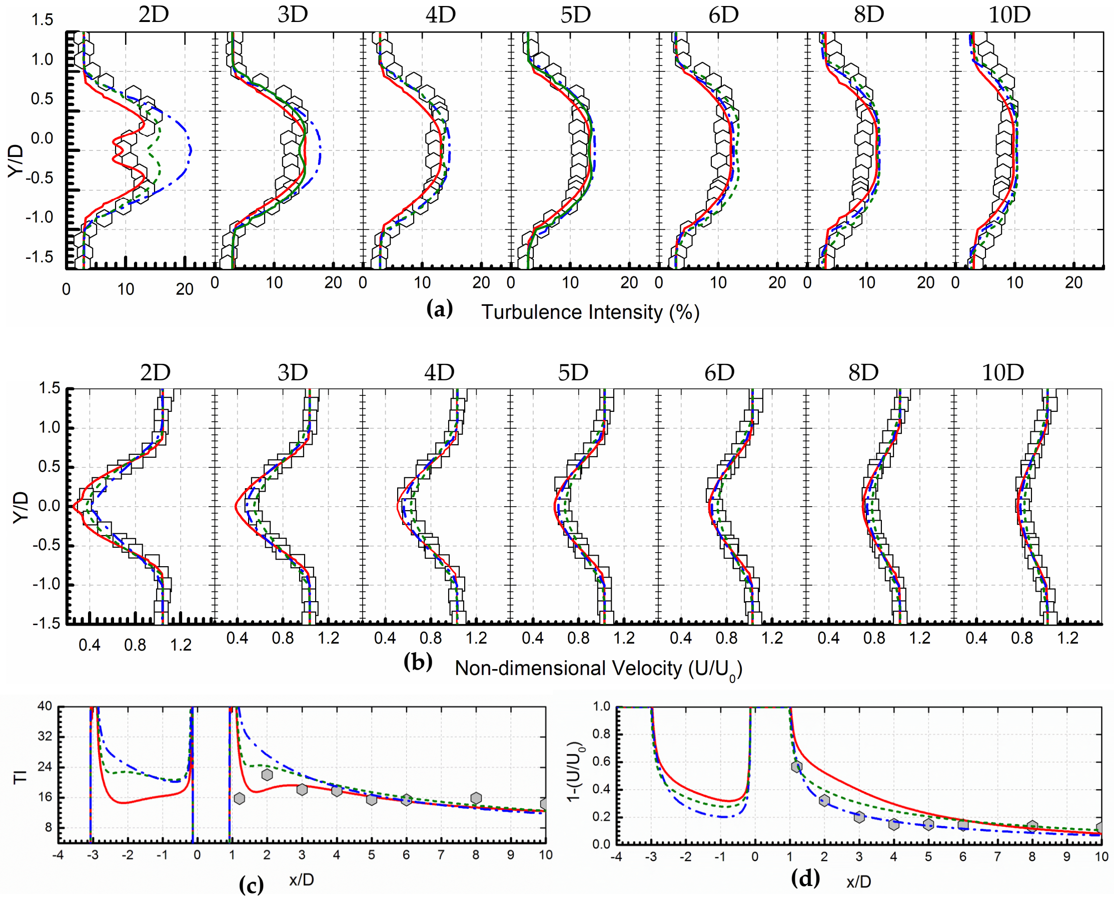

Figure 2: TI profiles (a) and velocity deficit (b) along the rotor center for the IFREMER's double rotors case TI=3% and 4D spacing, TI profiles (c) and velocity deficit (d) along the rotor center. ⬡: TI from the experiment [1], □: U/U_0 from the experiment [2], - - -: Corrected k-w results, - — - —: k-w model results ——: SST model results.

URANS simulation- Manchester rotor test

A group of experiments for three rotors operating in turbulent upstream are studied by Stallard et al. [2]. The experimental are carried out in the flume (test section: 5m width, 12m length, 0.45m depth) at University of Manchester. The turbulent inlet flow is characterized by mean velocity $U_\infty = 0.47m/s$ and $I_\infty = 10\%$ at the rotor plane for the experiment. All of the three rotors are operated under TSR=4.7.

Figure. 3 shows the wake profiles of normalized mean velocity and TI at 6 transects (2D~12D). It is evident that the major differences of the three turbulence models are in the range of x/D < 4. The $k-\omega$ model over-predict TI and under-predict the velocity deficit from 2D to 4D. $k-\omega$ model cannot predict the double TI peak induced by the tip at x = 2D. The *SST* model shows the best prediction of TI, however the velocity still recovers too fast at the rotor center. For the near wake ($x \leq$ 2D) prediction, the performance of corrected $k-\omega$ model is better than the $k-\omega$ but worse than the *SST* model. While for the far field wake (12D ≥ x ≥ 6D) prediction, results of all three models confirm with the experiment. For the high TI case, the wake merging can be observed evidently in the numerical and experimental tests. The differences of three wakes cannot be distinguished when x ≥ 8D.

LES simulation-Gravity based tidal current turbine

Lastly, the AL/MLS-IB method is extended to LES simulation of a gravity based tidal turbine, as shown in Figure 4 (a).

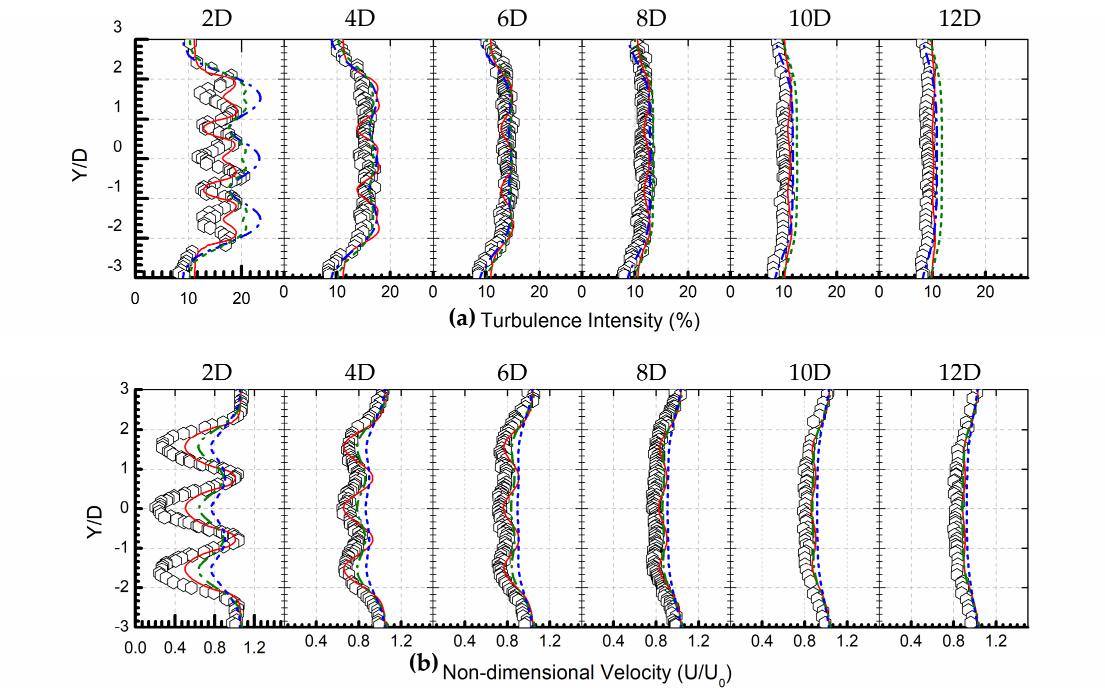

Figure 3: Wake profiles for the Manchester's triple rotors case with inlet turbulence intensity of 10%, the spacing of two rotors is 1.5D, same description of the symbols and lines can be found in Figure. 2.

The dynamically cell-based mesh refinement in OpenFOAM is utilized to resolve the regions containing solid surface and large velocity gradient. Figure 4 (b) and (c) demonstrate the mesh before or after the rotation starts, respectively. The regions adjacent to the support structure and blades as well as tip vortex are under refining (Figure. 4(d)).

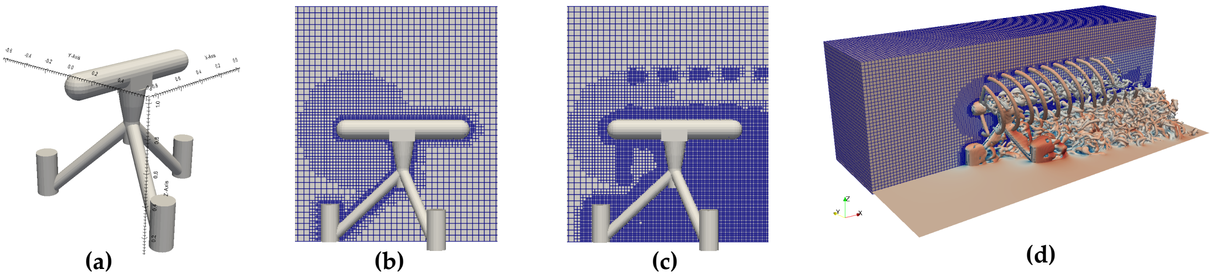

Figure 4: (a) Structure of a gravity based tidal current turbine, (b) and (c) indicate the initial and instantaneous adaptive mesh during the simulation, (d) instantaneous vortex structure and adaptive mesh.

Summary

In this manuscript, we present our numerical developments on prediction of the wake induced by the tidal turbine rotors. This study is based on our previous study on the IB method [5] [6]. Several tests show that the present AL/MLS-IB method is efficient and accurate to predict the wake of multiple tidal turbines.

References

[1] Mycek P, Gaurier B, Germain G, et al. Experimental study of the turbulence intensity effects on marine current turbines behaviour. Part II: Two interacting turbines. Renewable Energy, 2014, 68: 876-892.

[2] Stallard T, Collings R, Feng T, et al. Interactions between tidal turbine wakes: experimental study of a group of three-bladed rotors. Philosophical Transactions of the Royal Society of London A: Mathematical, Physical and Engineering Sciences, 2013, 371(1985): 20120159.

[3] Sørensen J N, Shen W Z. Numerical modeling of wind turbine wakes. Journal of Fluids Engineering, 2002, 124(2): 393-399.

[4] Vanella M, Balaras E. A moving-least-squares reconstruction for embedded-boundary formulations. Journal of Computational Physics, 2009, 228(18): 6617-6628.

[5] Liu C, Hu C. An adaptive multi-moment FVM approach for incompressible flows, Journal of Computational Physics, 2018, 359, 239-262.

[6] Liu C, Hu C. An efficient immersed boundary treatment for complex moving object. Journal of Computational Physics, 2014, 274: 654-680.